New Journal of Physics
The open access journal at the forefront of physics

Deutsche Physikalische Gesellschaft DPG IOP Institute of Physics

PAPER • OPEN ACCESS

Computing rotational energy transfers of OD^-/OH^- in collisions with Rb: isotopic effects and inelastic rates at cold ion-trap conditions

To cite this article: L González-Sánchez *et al* 2015 *New J. Phys.* **17** 123003

New Journal of Physics
The open access journal at the forefront of physics

Deutsche Physikalische Gesellschaft DPG
IOP Institute of Physics

Published in partnership with: Deutsche Physikalische Gesellschaft and the Institute of Physics

OPEN ACCESS

RECEIVED
21 July 2015

REVISED
16 October 2015

ACCEPTED FOR PUBLICATION
9 November 2015

PUBLISHED
4 December 2015

PAPER

Computing rotational energy transfers of OD^-/OH^- in collisions with Rb: isotopic effects and inelastic rates at cold ion-trap conditions

L González-Sánchez[1], F A Gianturco[2,3], F Carelli[2] and R Wester[2]

[1] Departamento de Química Física, Universidad de Salamanca, Pza. de los Caídos sn, E-37008, Salamanca, Spain
[2] Institut für Ionenphysik und Angewandte Physik, The University of Innsbruck, Technikerstr. 25, A-6020, Innsbruck, Austria
[3] Scuola Normale Superiore, Pzza de Cavalieri 7, I-56126, Pisa, Italy

E-mail: francesco.gianturco@uibk.ac.at

Keywords: MOT traps, collisional energy transfer, cold ionic collisions

Abstract

We report close-coupling (CC) quantum dynamics calculations for collisional excitation/de-excitation of the lowest four rotational levels of OD^- and of OH^- interacting with Rb atoms in a cold ion trap. The calculations are carried out over a range of energies capable of yielding the corresponding rates for state-changing events over a rather broad interval of temperatures which cover those reached in earlier cold trap experiments. They involved sympathetic cooling of the molecular anion through a cloud of laser-cooled Rb atoms, an experiment which is currently being run again through a Heidelberg–Innsbruck collaboration. The significance of isotopic effects is analysed by comparing both systems and the range of temperatures examined in the calculations is extended up to 400 K, starting from a few mK. Both cross sections and rates are found to be markedly larger than in the case of OD^-/OH^- interacting the He atoms under the same conditions, and the isotopic effects are also seen to be rather significant at the energies examined in the present study. Such findings are discussed in the light of the observed trap losses of molecular anions.

1. Introduction

The study of molecular collisions at low temperatures has witnessed very substantial advances in the last few years because of the great variety of areas, both fundamental and applied, in which they can play a role and help us to further understand the specific quantum features of the events observed. Such features indeed become increasingly more evident as the systems' temperature is reduced down to its lowest possible values [1–3].

Thus, observing molecular collisions at very low temperatures, from a few kelvins and down to millikelvins, has found many applications ranging from fundamental precision measurements [4], quantum information processing [5], quantum controlled chemistry [6] and the molecular process of the cold interstellar medium [7].

Molecular ions have also played a prominent role in these investigations and therefore a variety cooling schemes have been developed to produce specific molecular systems in their lowest vibrational and rotational internal levels [8–10]. The importance of such different procedures rest on their capability of manipulating and preparing molecular ions which can then be used further on, and within state-controlled molecular processes, with reactive partners [11].

It has therefore been made evident in this specific area that translational temperatures as low as a few millikelvins can be obtained by sympathetically cooling the molecular ions using laser-cooled atomic ions which are jointly confined in a radiofrequency trap [10]. The existing long-range interactions, on the other hand, will prevent the molecular ions prepared within such setups to also achieve internal cooling of their quantum states.

Another possible alternative which has also been considered involves using cold neutral atoms which can thus more efficiently exchange energy with the initially trapped molecular ions by having closer collisional encounters in the trap: the use of standard cryostats which employ He as a coolant is however limited to temperatures above about 4 K [12].

The next step in this search for an increasingly more efficient way to cool molecular ions has therefore been provided by the presence of hybrid-atom-ion-traps, whereby laser-cooled neutral atoms have been employed to further reduce the internal temperatures of molecular ions [13]. In such arrangements, therefore, a radiofrequency trap is superimposed with a magneto-optical trap (MOT) which then allows the molecular ions to be immersed in a cloud of laser-cooled heavier atoms, which can in turn collisionally cool internal degrees of freedom in the translationally cold molecular ions [14].

It has become apparent rather quickly, however, that one needs to locally achieve efficient collisional conditions in order to be able to obtain the internal molecular cooling step as rapidly as possible. Thus, recent experiments [15] have already been discussing the behaviour of a specific molecular anion (OH^-) interacting with a cloud of laser-cooled Rb atoms and managed to preliminary show the achievement of a relative temperature of 400 $\pm$ 200 K. Furthermore, very recent experiments on the same molecular ion, but this time made to interact with He atoms [16], have definitely been able to show that an efficient cooling of internal rotational levels of the OH^- ionic partner at a relative temperature of about 15 K is occurring within the trap.

Within both setups, it was already made clear by those studies that a direct knowledge of the partial collisional cross sections for the collisional changes of rotational quantum levels of the OH^- partner with either He or Rb atoms is a necessary ingredient for the understanding of the kinetic network that ultimately controls the final populations of $j = 0$ molecular ions. Another interesting piece of information extracted from those experiments, and needing the possible verification from direct quantum calculations, has been the comparison in size and T-dependence of the various rates observed for either OH^- or OD^-. In other words, the investigation of isotopic effects.

To study this end, we therefore investigate in this work the consequences of isotopic change for OH^-/OD^- systems in collision with cold Rb atoms. Since we have already looked at such effects for the case of the He atoms as collisional partners [16], we wish to extend that study to the present system and additionally reach the temperature conditions of the existing experimental data. Therefore, in the present calculations we also intend to link the possible experimental outcomes to be achieved down to a few kelvin (and currently carried out in an Heidelberg and Innsbruck collaboration [17]) with the preliminary experiments that have already obtained temperatures around 200–400 K [15]. To do so, it therefore becomes necessary to extend calculations to much higher energies than previously done for this system [18]. The following section therefore briefly outlines the features of the interaction potential, as obtained from earlier *ab initio* calculations. It also summarises the computational details for generating the partial inelastic cross sections, and the corresponding rates for temperatures ranging from a few K to 400 K.

The results for the OD^--Rb system are presented in section 3 and compared with the OH^--Rb system. Conclusions are presented in the section 4.

2. The computational tools

2.1. The *ab initio* potential

The ground-state electronic structure of the $RbOH^-$ system is given by the interaction between the OH^- electronic ground state with term symbol $^1\Sigma^+$ and the neutral rubidium atom, the ground state of which is represented by $^2S_{1/2}$. It thus follows that the linear configuration of the complex has a term symbol of $^2\Sigma^+$. Since we are considering the target molecule to be a rigid rotor in its ground vibrational state, the spatial features of that electronic interaction have been described by two Jacobi coordinates only (R,Θ, r_{eq}). Here r_{eq}, indicating the equilibrium geometry of the anionic partner, was taken to be 0.79 Å and the variables (R, Θ) were used on a discrete grid within the radial interval of (1.9–18.00) Å, with a variable length of the radial step (see [18, 19] for further details). The angular variable ranged, as expected, over the [0°–180°] interval with $\Delta\Theta = 15°$.

The *ab initio* calculations involved an all-electron correlation treatment with the exception of the ($^1S^2$) oxygen core. The restricted coupled-cluster with singles, doubles and non-iterative triples method was used and we employed a basis set of aug-cc-pVQZ for H and O atoms. The Rb atom was treated within the effective core potential approach, in order to reduce the number of electrons which were explicitly included but to still account for the relativistic effects in the core electrons; both the type of the effective-core potential and the basis set chosen for the description of the rubidium atom were taken from [20]. All the computational details are given in [19], while we present here simply an overall view of those results to better explain and discuss the ensuing dynamics of the quantum collisions. Just as a further reminder, in the calculations we followed the full counterpoise procedure [21] to account for the effects of basis set superposition errors.

The 3D plot of the potential energy surface (PES) of the title system provides useful information on the overall features of the interaction potential: it is obvious from [18, 19] that the (OH^--Rb) complex gives rise to a strongly bound system. The global energy minimum is located on the side of the oxygen atom, for $\Theta = 180°$ in our representation, at a distance from the centre-of-mass (c-o-m) of 2.44 Å: it carries a minimum energy value

of 1.65×10^4 cm^{-1} which is clear indication of the presence of a strong chemical bond. The overall PES is also strongly anisotropic (i.e. Θ-dependent) and exhibits a second, minimum for $\Theta = 0°$ that is still well marked but smaller than that of the other linear configuration: 6.27×10^3 cm^{-1}. Since the OH^- carries a negative charge and a permanent polarisable moment, and the Rb atom can be viewed as a polarisable dielectric, we further had to generate the needed long-range expansion:

$$V_{LR}(R, \Theta) = C_{4,0}\frac{f_d(R)}{R^4} + C_{5,1}\frac{f_d(R)}{R^5}\cos\Theta \quad (1)$$

In (1) $f_d(R)$ describes radial damping functions which are used to extend the 2D-fitting to the external radial regions. The $C_{4,0}$ coefficient is linked to the Rb polarisability, α_0, of ~46.64 Å^3, not far from the experimental value of 47.4 ± 0.9 [22]. The additional dipole-polarisability term is included via the following expression:

$$C_{5,1} \sim 2\alpha_0\mu \quad (2)$$

which, when using the previous value of the polarisability, produces a fitted dipole value of 0.553, not far from the *ab initio* value of 0.566 au [18].

2.2. The multichannel quantum dynamics

The OH^-/OD^- molecules exhibit, for their lowest rotational levels, the relative energy spacing reported already in [18], and which we shall further discuss later on. Suffices it to say for now that, in going from the OH^- rotor to the OD^- rotor, the $j = 1$ level changes by 17.17 cm^{-1}, while the $j = 2, 3$ and 4 reduce their respective spacings in the following ways: $\Delta j(1 - 2) = 74.28$ cm^{-1} for the OH^- and 39.94 cm^{-1} for the OD^-; the $\Delta j(2 - 3) = 111.42$ cm^{-1} for the OH^- and 59.91 cm^{-1} for the OD^-; while the $\Delta j(3 - 4) = 148.56$ cm^{-1} for the OH^- and 79.87 cm^{-1} for the OD^-. On the whole, therefore, the mass effect which occurs in going from OH^- to OD^- reduces the rotational spacings by marked, and relatively important, energy amounts. The effects of such changes on the overall state-to-state dynamics will become evident from the results we shall report in the following sections.

To handle the quantum dynamics we specifically employed the time-independent (TI) formulation of the quantum scattering of a neutral atom (Rb) off a spherical rotor (OH^-/OD^-) following the general discussion of this problem already detailed by us in our earlier work [18, 19, 23]. In the present, we shall only provide a brief outline of its in-house implementation.

The TI scattering state of a system of interacting partners can be expanded in terms of diabatic (asymptotic) target eigenstates:

$$\Psi^{i,+}(R, \underline{x}) = \sum_f F_{i\to f}(R) \times X_f(\underline{x}). \quad (3)$$

Here i labels the (collective) initial states of the colliding partners and the X_f are the eigenstates of the isolated molecule (channel eigenstates). The $F_{i\to f}$ are the channel components of the scattering wavefunction which have to be determined by solving the Schrödinger equation subject to the usual boundary conditions

$$F_{i\to f}(R) \to \delta_{if}h^{(-)}(R) - S_{if}h^{(+)}(R) \quad \text{as} \quad R \to \infty, \quad (4)$$

where f denotes a channel which is asymptotically accessible at the selected energy (open channel) and $h^{(\pm)}$ is a pair of linearly independent free-particle solutions. Usually, numerically converged scattering observables are obtained by retaining only a finite number of discrete channels in (3). One thus gets a set of M coupled differential equations for the $F_{i\to f}$ unknowns (which form a matrix solution $\mathbf{\Psi}$) subject to the regularity conditions of each solution at the origin ($F_{i\to f}(0) = 0$) and to the boundary conditions given by (4).

In the case where no chemical modifications are expected to be energetically accessible for the target by the impinging atom (as is in our present analysis: see further discussion below), the total scattering wavefunction can be expanded in terms of asymptotic target rotational eigenfunctions (within the rigid rotor approximation) which are taken to be spherical harmonics and whose eigenvalues are given by $Bj(j + 1)$. Here the B value was taken to be 18.5701 cm^{-1} for the OH^- and 9.98459 cm^{-1} for the OD^-. The channel components of (3) are therefore expanded into products of total angular momentum eigenfunctions and of radial functions. These radial functions are in turn the elements of the solutions matrix which appear within the familiar set of coupled, second order homogeneous differential equations:

$$\left\{\frac{d^2}{dR^2} + \mathbf{k}^2 - \mathbf{V} - \frac{\mathbf{l}^2}{R^2}\right\}\mathbf{\Psi} = 0, \quad (5)$$

where $[\mathbf{k}^2]_{ij} = \delta_{ij}2\mu(E - \epsilon_i)$ is the diagonal matrix of the asymptotic (squared) wavevectors and $[\mathbf{l}^2]_{ij} = \delta_{ij}l_i(l_i + 1)$ is the matrix representation of the square of the orbital angular momentum operator. This

matrix is block-diagonal with two sub-blocks that contain only even values of $(l' + j')$ or only odd values of $(l' + j')$.

One now further defines the additional LogDerivative matrix $\mathbf{Y} = \mathbf{\Psi}'\mathbf{\Psi}^{-1}$, where primed denotes derivatives with respect to R which satisfy the well-known Riccati matrix equation

$$\frac{d\mathbf{Y}}{dR} + \mathbf{W} + \mathbf{Y}^2 = 0 \tag{6}$$

in which $\mathbf{W} = \mathbf{k}^2 - \mathbf{V} - \mathbf{l}^2/R^2$ is a term containing the potential matrix $\mathbf{V}$. The scattering observables are obtained in the asymptotic region where the LogDerivative matrix has a known form in terms of free-particle solutions and unknown mixing coefficients. For example, in the asymptotic region the solution matrix can be written in the form

$$\Psi(R) = \mathbf{J}(R) - \mathbf{N}(R)\mathbf{K}, \tag{7}$$

where $\mathbf{J}(R)$ and $\mathbf{N}(R)$ are matrices of Riccati–Bessel and Riccati–Neumann functions. Therefore, at the end of the propagation one obtains the $\mathbf{K}$ matrix by solving the following linear system

$$(\mathbf{N}' - \mathbf{Y}\,\mathbf{N})\mathbf{K} = \mathbf{J}' - \mathbf{Y}\,\mathbf{J} \tag{8}$$

and from the $\mathbf{K}$ matrix one gets easily the S-matrix and the cross sections. We have recently published an algorithm that modifies the variable phase approach to solve that problem, specifically addressing the latter point [24] and we defer the interested readers to that reference for further details on our computational implementation.

In the present calculations, therefore, we have used multipolar potential terms up to $\lambda_{\max} = 9$ in (9)

$$V(R, \Theta) = \sum_{\lambda} V_\lambda(R) P_\lambda(\cos\theta) \tag{9}$$

Here the $V_\lambda(R)$ describe the relative strength of the anisotropy for each multipolar term. We have extended the radial range of integration out to 15 000 Å using a total of 30 000 integration steps. The maximum number of total angular momentum values was extended up to $J_{\max} = 250$, while the number of rotational channels always included at least 15 closed channels above the last open channel at the given collision energy. The accuracy of the above fitting of the *ab initio* raw points ranged from a few wavenumbers in the well regions and the long-range parts to about 10 wavenumbers in the repulsive walls regions. The above parameters' choices turned out to be sufficient for both types of isotopic molecular anions.

3. Results and discussion

3.1. OH^- collisions with Rb at higher energies

As we have extensively discussed in the introduction section, detailed information on the size of the state-to-state internal energy transfer efficiencies by collisions under trap conditions is one of the important ingredients for understanding the likely values of the internal temperatures of the trapped ions, as well as the possible paths of molecular losses by evaporation from the traps. Hence, to generate the corresponding rotational de-excitation (and also excitation) rates by collisions requires to computationally sample a fairly large range of energies for all the processes expected to be involved.

More specifically, in our present study for the ions confined in cold traps, and undergoing sympathetic cooling with laser-cooled Rb atoms, we shall analyse first the earlier experiments [15], where the reached trap temperature was estimated around 400 ± 200 K. By further looking at these processes at lower temperatures we shall make contact with the current experiments which, at least in principle, plan to cool this molecular anion, in the trap with Rb atoms, down to a few kelvins [17].

To be able to provide indications on the rotational state-changing rates that involve the lowest rotational levels (e.g. $j = 0, 1, 2, 3$) and occur with molecules which are taken to be already in their ground vibrational level $v = 0$ [15–17], we now need to extend our earlier calculations for the OH^--Rb system [18] to higher energies in order to obtain final, inelastic rates up to 400 K. The latter constitutes the controlling temperature for which the state-changing cross sections will be needed: it requires energy values up to about 3000 cm^{-1}.

The excitation cross sections involving rotational levels for $j = 0, 1, 2$ and 3 are reported by figure 1, where all the individual inelastic processes are indicated up to a relative collision energy of 1000 cm^{-1}. The further extension up to 3000 cm^{-1} is reported for all the states involved within the inset of the same figure.

The energy-dependence for these computed cross sections shows their rapid drop in value when the collision energy is increased: we see, in fact, that for an energy increase from about 50–200 cm^{-1}, the $(0 \rightarrow 1)$ cross sections decrease by a factor of almost five, while the other cross sections also decrease very drastically. Thus, at the highest energy reached by the calculations in the main panel (1000 cm^{-1}) and for their further increase out to 3000 cm^{-1} which is being reported in the inset, all the $\Delta j = 1$ cross sections are down in size to below about

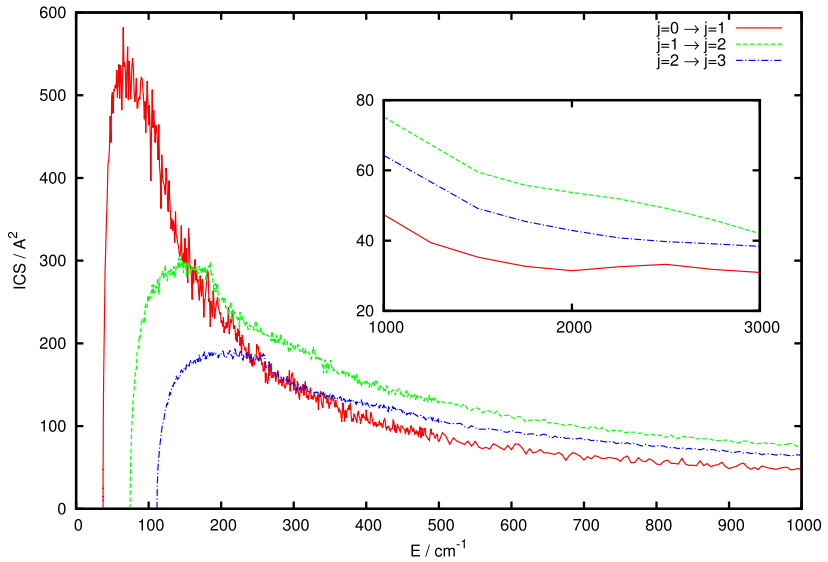

Figure 1. Computed state-to-state excitation inelastic cross sections from initial rotational levels of OH^-. All transitions between $j = 0$ and $j = 3$ are considered for the excitation channels. The inset shows the same cross sections at the higher energy considered in this work. The colours online are labelling the different transitions.

50 Å^2: this is a reduction in size of nearly one order of magnitude, at least for the $(0 \rightarrow 1)$ process. This result therefore tells us that the excitation processes in cold traps will be the most efficient when the trap temperature will be reduced down to its lowest expected values around 20–30 K, as extensively discussed in [18]. The internally 'hot' molecules would therefore have to relax to their ground state by heating the environmental gas by collision.

If we now turn to the de-excitation (internally 'cooling') transitions, reported in the main panel of figure 2, we see once more the dramatic effects which take place when increasing the collision energies for which the state-changing dynamics is being analysed: the $\Delta j = -1$ processes from $j = 1, 2$ and 3 levels decrease several orders of magnitude from a few cm^{-1} up to 500 cm^{-1}. They all decrease down to about 30 Å^2 when the collision energies reach 1000 cm^{-1} and all become uniformly well below 20 Å^2 as we reach 3000 cm^{-1} of collision energies. Thus, at low-T this system also show efficient de-excitation of its rotational levels by collision with the cold Rb gas.

For both types of processes, therefore, the new calculations at higher energies tell us that the sizes of the relative cross sections markedly change as the collision energy increases. On the other hand, one should also note that they still remain much larger than those for the case of OH^- collisions with He [16], where the cross sections up to 1000 cm^{-1} were only around 10 Å^2. Since those values turned out to produce rotational de-excitation rates that were sufficiently large to bring down to its ground state the trapped OH^- ions [16], we argue now from the present calculations that for this system the collisional 'rotational cooling' can occur even before the ions would leave the trap. This therefore means that, as in the case of $OH^- + He$, the OH^--Rb combination should also efficiently 'cool' the anion's rotational level populations under trap conditions.

In order to verify the above suggestion more closely we have therefore computed the corresponding rotational de-excitation rates at the higher temperatures of the ion trap obtained by the earlier experiments on this system [15]. We have carried out additional calculations for the corresponding state-changing rates by a convolution over the Boltzmann's distribution of relative velocities at the trap's translational temperature

$$k_{j\rightarrow j'}(T) = \left(\frac{1}{\pi\mu}\right)^{1/2}\left(\frac{2}{k_B T}\right)^{3/2}\int E\sigma_{j\rightarrow j'}(E)\exp\left(-E/k_B T\right)\mathrm{d}E. \qquad (10)$$

Here k_B in the Boltzmann's constant, E the relative collision energy and T the trap's translational temperature.

We have calculated the above rates from a few kelvins up to 400 K of trap temperature and employing $\sigma_{j\rightarrow j'}(E)$ values up to 3000 cm^{-1}. For the integration's convergence we started with E values above threshold by about 10^{-3} cm^{-1} and employed for each $k_{j\rightarrow j'}$ rate a unevenly spaced number of energy values which ranged up to a total of over a thousand. Numerical convergence was thus checked to be better than 10^{-2}.

The experiments described in [15] indicate that, at the expected temperatures of their trap (400 ± 200 K) the inelastic rate coefficient for trap losses was estimated to be $(2^{+1}_{-1})\cdot 10^{-10}$ cm^3 s^{-1}. The possible origins of these rate coefficients for loosing OH^- ions from the trap were linked to the known mechanism of associative detachment (AD):

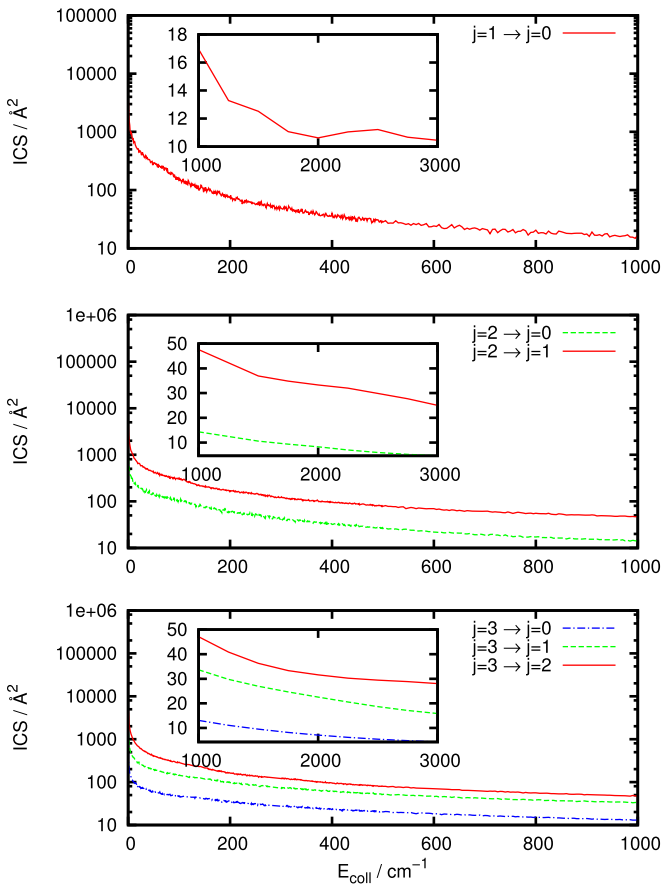

Figure 2. Computed rotational de-excitation (internal 'cooling') collisional cross sections over the same range energies of figure 1, for state-changing processes from the first three levels with $j > 0$. See text for further details.

$$OH^- + Rb \rightarrow RbOH + e^- \quad (11)$$

which has been estimated to be exothermic by 1.4 eV [25, 26]. However, recent model calculations regarding the above process [27] suggested that the AD channels would be open only if the OH^- ions in the trap were vibrationally excited to $v \geqslant 2$, since no appreciable AD rate coefficients were found for vibrationally colder molecules. However, given the fairly simple modelling of the AD kinetics discussed in that work [27], the question of the actual role of the process of (11) in the existing experiments still remains to be answered and further calculations would be needed to settle its mechanism and its efficiency under trap conditions. At the present stage, therefore, our results do not include the AD channels in the rate calculations since we assume, from what stated by the experiments, that all molecular anions populate the ground vibrational level and therefore the AD process is probably still closed. We now present in figure 3 the state-to-state behaviour of the rotational de-excitation collisional rates up to the expected temperatures of the experiments in [15]. One should keep in mind that on rotationally 'cooling' the molecular partner, the released energy enters the bath and therefore gets redistributed between partners. Given the lighter mass of the molecular anion, the latter is then more likely to translationally 'heat up' in comparison with the Rb atom, thereby leaving the trap.

The data in that figure clearly show that the individual, partial rotational de-excitation rates for the lowest three excited states of OH^- in the trap have a rather slow dependence on temperature: from 50 to 450 K, each rate changes at most by a factor of 2 or less. The range of values spanned by all the rates covers about one order of magnitude: all of them are defined roughly between 10^{-10} cm^3 s^{-1} and 10^{-9} cm^3 s^{-1}. We also see that the most efficient rotational de-excitation transitions are those from the more excited OH^- partners: from $j = 3$ and $j = 2$. With the same token, de-excitation processes with $\Delta j > -1$ yield rates of smaller sizes, as expected (see earlier discussion at lower T in [18]).

In order to provide a more global evaluation of the collisional 'rotational internal cooling' efficiency, we have further modelled the rotational distribution of OH^- states in the trap as being a Boltzmann-like distribution at each considered temperature. Hence we have examined such global indicators from $T = 200$ to 450 K, a range that spans the experimental findings on trap temperatures of the earlier measurements [15]. We have then summed the computed rates by weighting each of them with the relative distribution coefficients and at each T values.

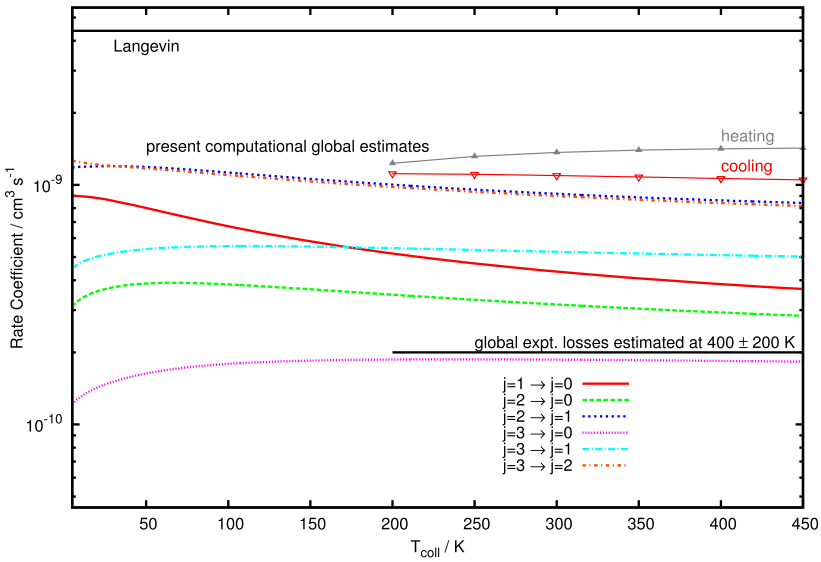

Figure 3. Computed rates for rotational internal 'cooling' of OH^- in collisions with Rb atoms, over the range of temperatures up to those sampled in the experiments. All down transitions from the first four rotational levels are considered. The different processes are labelled both by colours online and by the different line markings given in the figure. The global 'heating' and 'cooling' labels in the figure refer only to the internal rotational level population of the molecular anion. They are estimated as described in the main text.

The results are reported in the same figure 3 by the curve marked with filled-in triangles and conventionally indicated by 'heating' or 'cooling', a simplified labelling referring only to the state of the internal rotational level population of the anionic partner molecule after collisions. One clearly sees there that, as expected, the global rotational de-excitation rates also depend very little on T and remain close to the value of 1.06×10^{-9} cm^3 s^{-1}. This is a rather efficient collisional de-excitation process of OH^- partners in the trap with Rb: we therefore expect that this molecular system could rapidly be brought down to the $j = 0$ level before leaving the trap through some other loss process. One should also keep in mind, as mentioned earlier, that internal rotational de-excitation processes actually increase the translational 'heating' of the bath. Since the molecular anion is the lighter collisional partner, one also would expect that its translational temperature would increase more and would also contribute to trap losses. In fact, the experimental estimate on inelastic losses (also shown in the figure) are very similar in size to our global value, a result which allows us to make the following considerations:

(i) rotational de-excitation collisional efficiency could cause possible trap losses of the molecular anion in the setup of the experiments in [15], although it was not explicitly considered in that study,

(ii) not much is known about vibrational heating rates in such traps, although the OH^- molecules are expected to be largely in their $v = 0$ level. On the other hand, our earlier numerical estimates of vibrational inelastic processes in another ion, MgH^+, internally vibrationally de-excited in cold traps by buffer cooling via He gas [28] indicated that such rates would be between two and three orders of magnitude smaller than their rotational cooling counterparts;

(iii) one could therefore surmise that the large values of the global losses found in the experiments, which are of the same order of magnitude as our present rotational cooling rates, could be possibly due either to the presence of active AD channels as those described by (11) or to translationally heated molecules which can leave the trap.

To further extend the present analysis of the efficiency involving the lower rotational levels of this molecular anion (taken to be also in its $v = 0$ level), we present in figure 4 the corresponding behaviour of the rotational excitation rates for the OH^- partners in the sympathetic trap with Rb atoms. The rates shown involve collisional excitations from the $j = 0, 1, 2$ levels.

The computed excitation rates reported in the figure are seen to rapidly grow in size at each opening threshold, reaching their maximum values within about 50 K for the $\Delta j = 1$ excitation process. By the time the trap's temperature reaches about 300 K, we see in fact that all these excitation processes become comparable in size, reaching rate values around 1.0×10^{-9} cm^3 s^{-1}. On the other hand, the $\Delta j = 2$ and $\Delta j = 3$ transitions are associated with processes for which the rates reach around 400 K a lower, and nearly common, value of 0.5×10^{-9} cm^3 s^{-1}. In order to model somewhat more realistically the equilibration of relative populations

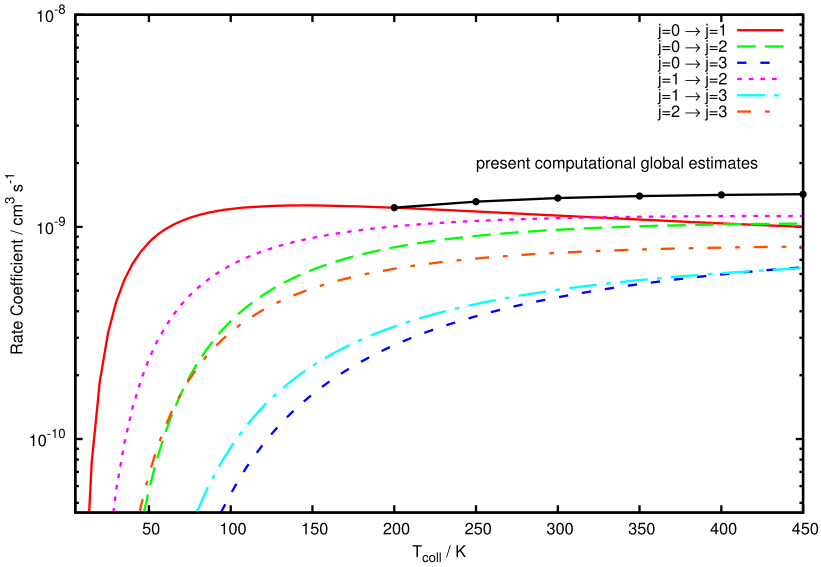

Figure 4. Computed rotational excitation rates for the title system with OH^-, over the range of temperatures reaching those sampled in the experiments. All 'internal heating' transitions from the first three rotational levels are considered. The global rotational excitation rates are estimated as described in the main text.

between the levels considered as active for the molecular anion in the trap, we have also carried out a Boltzman averaging of the excitation rates at the experimental trap temperatures: their values from about 200 K and up to 450 K are reported by the filled-in dot curve in the same figure 4. As a further comparison, we also report these values within the data of the earlier figure 3. The data indicate once more a slow dependence of the global 'internal rotational heating' within the range of temperatures considered, their overall value being around 1.2×10^{-9} cm^3 s^{-1}. Our present results also indicate a fairly high efficiency for the collisional state-changing rates of the anionic molecular partner in the trap with Rb atoms. The comparison with the corresponding estimates of the rotational de-excitation global rates of figure 3 indicates that both types of rotationally inelastic global rates are a factor of five larger than the estimated rate losses of the experimental conditions. Since our global rotational de-excitation rates could also cause, as we discussed before, losses of the molecular partner from the trap's environment, we could therefore argue that the translational heating of the bath in the trap originating from the 'rotational cooling' computed rates is a relevant contributor to the observed molecular losses from the trap. Our present computational findings also indicate that the internal state excitations by collision should be a very efficient path under the experimental conditions of the sympathetic cooling. It is also useful to look at the individual state-to-state processes involving the $j = 0, 1$ lowest rotational levels. From figure 3 we see that the rotational de-excitation rate is much larger than the corresponding rotational excitation rate in figure 4 up to about 50 K, thus suggesting that if the experiments with the Rb atoms could be brought down to the same temperature range as those carried out with He atoms [16], we should then expect that the molecular partner could be kept rather efficiently into its $j = 0$ ground rotational state.

3.2. Isotope effects for OD^- collisions with Rb under trap conditions

A further aspect of our present analysis deals with the effects on the size and energy dependence of the inelastic cross sections for the OD^- partner colliding with Rb atoms. To remind readers of the actual sequence of energy spacings we report in figure 5 a comparison between levels.

A quick perusal of the energy spacings of the two systems tells us that the lowest three excited rotational levels of the heavier isotopic variant cover roughly the same energy range (120 cm^{-1}) as the first two rotational levels of the lighter molecule. We therefore see that the reduction of the energy gaps during excitation/de-excitation collisions will be likely to cause marked differences among the corresponding cross sections. Such differences will be analysed below in more detail. The data of figure 6 report a comparison between relative sizes and energy dependence for the state-changing excitation cross sections from the lowest three rotational levels.

One of the differences between the two systems is the marked change in the threshold behaviour of the lowest excitation cross sections from the $j = 0$ initial levels. To reduce computational costs we have generated fewer points for the case of the heavier isotopic variant, so that changes in the resonance structures are harder to detect for the latter case. A more detailed analysis of resonance effects is outside the main scope of the present work, although we see much larger cross sections near threshold for the OD^- partner, this being so up to about

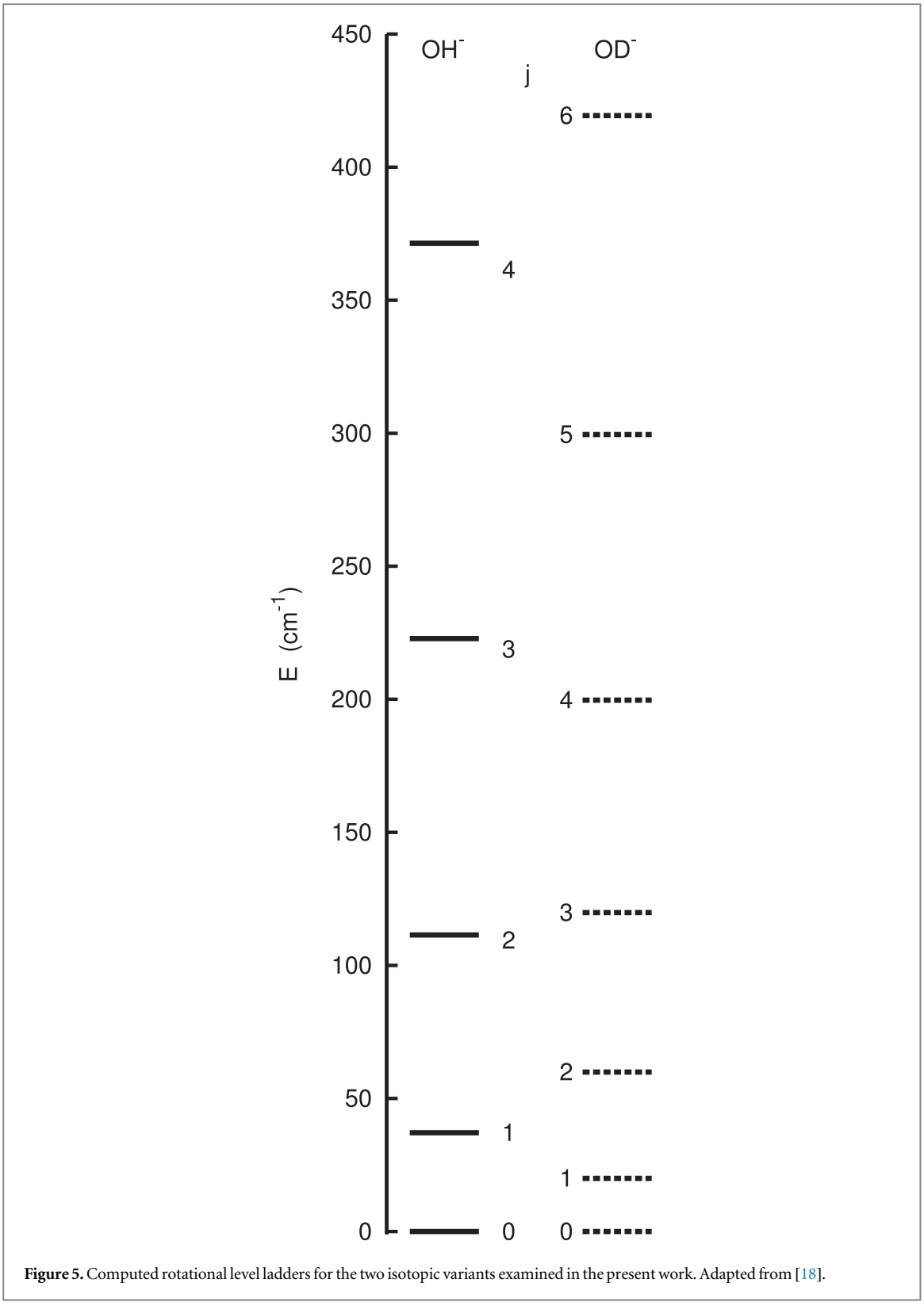

Figure 5. Computed rotational level ladders for the two isotopic variants examined in the present work. Adapted from [18].

50 cm^{-1}. On the other hand, as the collision energy increases the OH^- excitation process becomes more efficient and remains so up to the largest energy examined by us. Such an effect could be linked to features of the interaction PES that, for the present system, is exhibiting clear 'chemical' characteristics in the short-range region while being dominated by induction effects in the long-range region. Thus, the lower anisotropic multipolar coefficients are very important for near-threshold collisions and behave similarly for both isotopic variants. The heavier partner, on the other hand, involves smaller amounts of energy which are being transferred and therefore the reduced energy gap makes more probable its inelastic processes with respect to those of the lighter partner: this is seen in our results. As the collision energy increases, however, the dominant angular

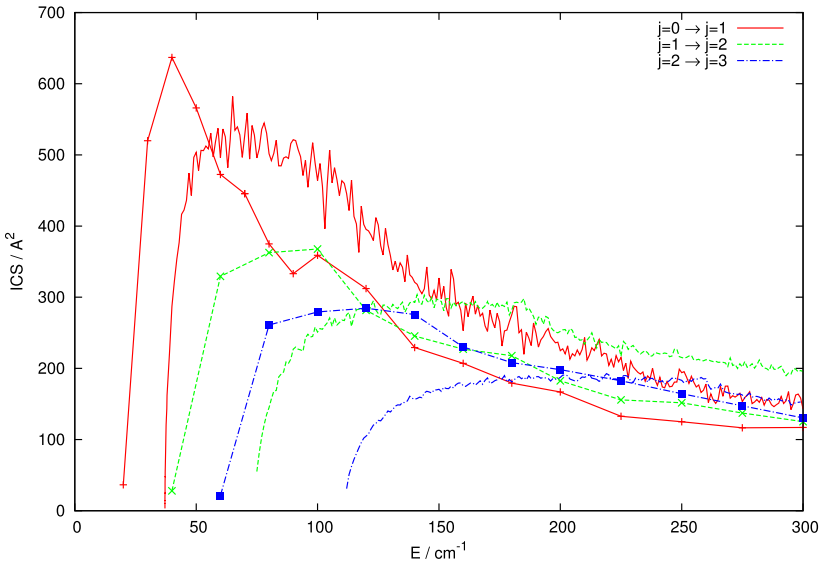

Figure 6. Computed rotational excitation cross sections for the two isotopic variants examined in the present work. All energy values are given in cm^{-1}. The heavier molecular ion's data are given by the curves further marked with crosses, with plus and with filled-in squares, while those for the lighter variant are given by the plain lines. Transitions are labelled as in the inset of the figure.

momenta for the OH^- partner are less than in the case of the OD^-, so that the former projectile penetrates more closely to the 'chemical' interaction regions than the heavier isotope. As a result, the coupling is more strongly controlled by the short-range potential features rather than by the simpler energy gap difference: the inelastic excitation cross sections therefore become larger for the OH^- than for OD^-. A very similar behaviour is also shown by all the other partial excitation cross sections reported by figure 6: the heavier isotopic system yields larger inelasticity at near-threshold energies, while the lighter OH^- produces larger inelastic cross section as the collision energy increases since more virtual levels are dynamically coupled in this case via the closer approaches of the lighter molecule: it thus samples the stronger, short-range region of the interaction. The computed partial cross sections for the de-excitation collisions involving the $\Delta j = -n$ (with $n = -1, -2$ and -3) processes from the $j = 1, 2, 3$ initial levels are reported by figure 7 in its three panels.

In the $\Delta j = -1$ de-excitation process, since no threshold energy is present, we see that the energy gap differences play an important role at all the energy considered, although the effects are much more marked at the lowest collision energies: these 'super-elastic' processes transfer more internal energy to the relative translational energies for the case of the lighter isotopic variant, thus reducing the interaction times for the lighter system in comparison with the heavier one. This feature makes the OH^- dynamics more 'sudden', and hence more efficient. Furthermore, we also see that the differences in potential-induced, dynamical couplings, which also depend on the number of trajectories involved in each case, become more important at the higher collision energies, thereby making the size of the two sets of quenching cross sections closer to each other (see panels in the figure 8). At the lowest collision energies, on the other hand, the rotational energy gap differences between isotopic variants dominate the long-range dynamics, thereby affecting the quenching efficiency differences between the two systems. The comparative behaviour of the other computed partial, state-to-state quenching cross sections is further reported in the other panels of the same figure 7.

The sets of calculations in these figures which involve the higher initial rotational levels show however a more complex interplay between effects of energy gap differences and importance of potential-induced dynamical effects. Thus, at the collision energies near the energy threshold the de-excitation efficiency of the lighter OH^- partner in the more excited initial states is much closer, and even smaller in some cases, to that for the cooling efficiency of the heavier isotopic variant, and remains so for energies up to a few milli-cm^{-1}: depending of the value of the Δj in the cooling transition, we see right at threshold the prevailing effects of either the energy gap factor or the varying strengths of the anisotropic potential-coupling factor. As the collision energies increase, however, we see that all the sets of cross sections for the lighter partner get to be clearly larger and remain so up to the largest energies: the coupling potential strength is now the dominant factor in driving the relative dynamics, as discussed earlier.

The data reported by figure 9 indicate the low-T behaviour of the rotation-quenching rates for the OD^- collisions with the Rb partner in comparison with those already discussed earlier for its lighter counterpart. The calculations cover the lower temperature region (up to about 35 K) which is expected to be the one likely to be finally reached in the ongoing experiments for the title system: in the figure we compare the present calculations

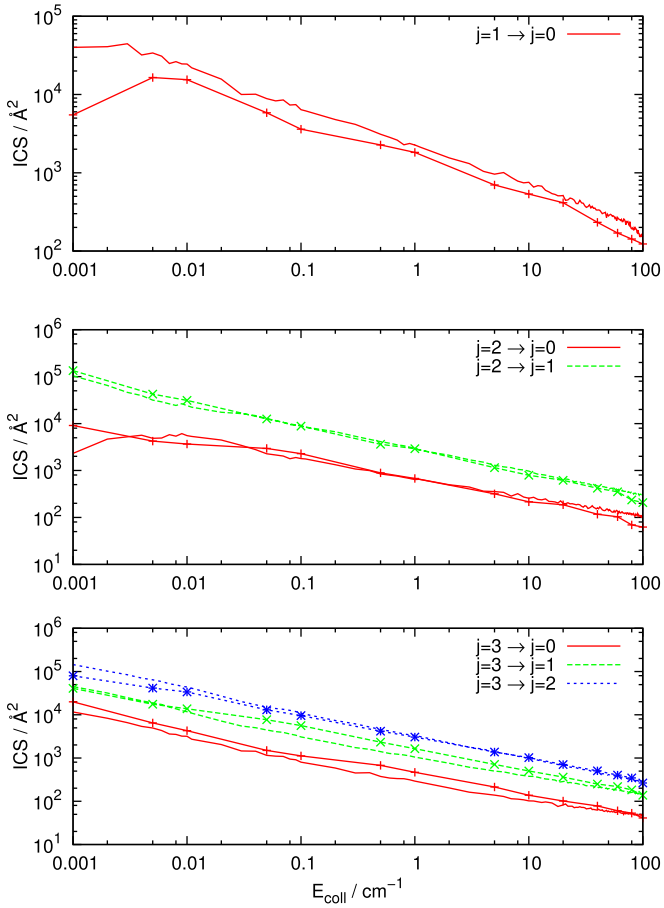

Figure 7. Computed rotational de-excitation cross sections for the two isotopic variants examined in the present work. All energy values are given in cm^{-1}. The heavier molecular ion's data are given by the curves further marked by crosses, while those for the lighter variant are given by solid, plain lines. The quenching process involves the $\Delta j = -1, -2$ and -3 transitions from the $j = 1, 2$ and 3 initial levels.

for the OD^- situation with those computed earlier by us for its lighter counterpart [18]. We see that, in general terms, the entire range of cooling processes considered here covers nearly one order of magnitude in size, varying from about 1.0×10^{-10} cm^3 s^{-1} at the smaller end to about 1.0×10^{-9} cm^3 s^{-1} at the larger end. Furthermore, we also see that the relative behaviour of the partial de-excitation cross sections discussed earlier is also reflected on the relative sizes of the corresponding rates: all rates for the lighter anion are invariably larger than those for the heavier counterpart since the partial cross sections for the former molecule have been shown to be larger at the threshold energies (see figure 7). On the other hand, the opposite occurs for the partial rates associated to the $\Delta j\,(3 - 1)$ and the $\Delta j\,(3 - 0)$: their corresponding partial cross sections were found to be larger for the heavier isotopic variant (see figure 8) and therefore the cooling rates at low-T are behaving the same way. Additionally, in the case of the $\Delta j\,(2 - 1)$ and the $\Delta j\,(2 - 0)$ quenching transitions, we see that the corresponding rates remain larger for the lighter partner in spite of the corresponding cross sections in figure 7 being at threshold larger for the heavier isotopic variant: in this case, in fact, the change in relative size between cross sections occurs at low enough collision energy to affect the corresponding rates at the considered temperatures. In other words, we see once more what we have discussed earlier in this section: the relative interplay of the dynamical and kinematics differences affects the relative sizes of the corresponding low-T rates, although in both cases such rates remain rather large and definitely larger than for the He collisional cooling rates discussed several times throughout the present paper.

4. Conclusions

In the present work we have analysed in detail the relative efficiency of the collisional state-changing partial cross sections for both OH^- and OD^- molecular anions in interacting with Rb atoms under cold trap conditions. We have employed an *ab initio* evaluation of the interaction forces [19] and carried out a rigorous, TI treatment of the multichannel quantum dynamics. The calculations have involved rotational excitation and corresponding

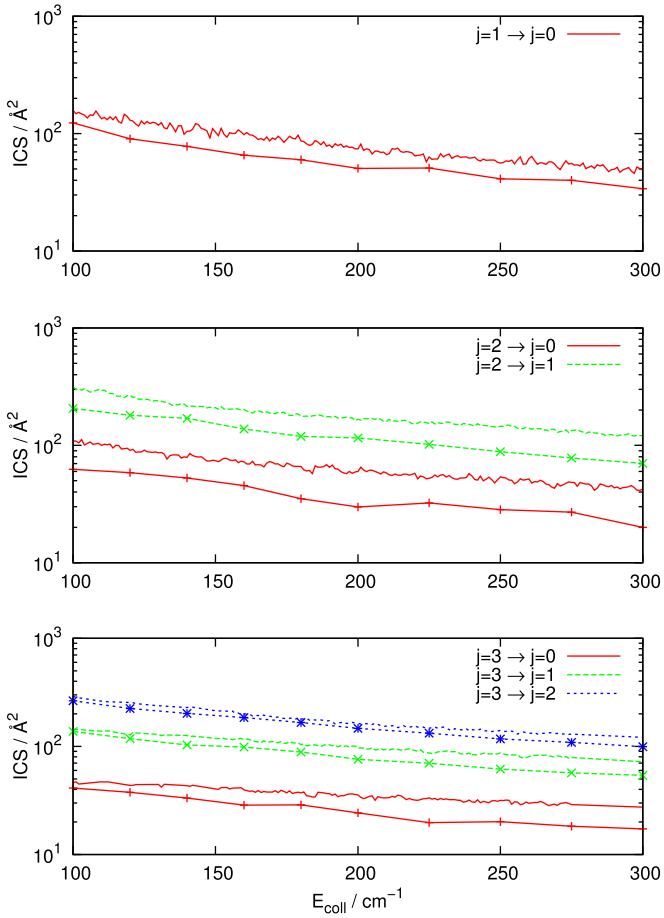

Figure 8. Computed rotational de-excitation cross sections for the two isotopic variants examined in the present work, this time at the higher collision energies with respect to figure 7. The heavier molecular ion's data are given by the curves which have further crosses as markings, while those for the lighter variant are given by plain lines. The transition labels are given by the colours and are also reported in the inset in the figure. The quenching process involves transitions from the $j = 1, 2$ and 3 initial levels for both systems.

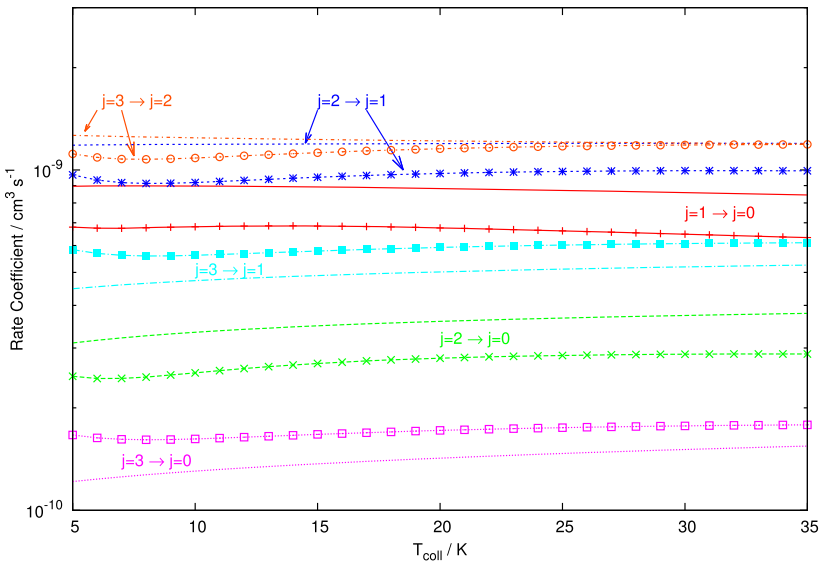

Figure 9. Computed rotational de-excitation rates of the two isotopic variants examined in the present work. The various lines with further markings refer to the heavier molecular anion, while the plain lines report calculations for the lighter isotopic variant. The markings of the various transitions are given by the inset within the figure. See main text for further details.

de-excitation for both systems. The transitions considered have dealt with the lowest four rotational states of the target molecules and the energy range for the analysis of isotopic effects has considered the possible experimental situations of future, colder MOT-hybrid traps which can be achieved via interaction with laser-cooled clouds of Rb atoms and operate around and below 30 K of temperature. The results have clearly shown that the rotational de-excitation of OH^- molecular anions is in general more efficient than that for its heavier isotopic counterpart, this being especially so at the higher collision energies, while the threshold behaviour of their respective de-excitation rates can change depending on the relative interplay of the strength of the potential-driven dynamics and the energy gap role in the transitions. The corresponding rotational excitation processes, on the other hand, indicate that the OD^- molecular partners are uniformly more efficiently excited at near-threshold energies while becoming less efficient as the collision energies increase. Such a behaviour could be linked to the interplay between dynamical coupling induced by potential anisotropic coefficients at the higher energies and the more important role played by the energy-gap differences at the near-threshold energies. Another aspect of the collisional state-changing dynamics which we have considered is the behaviour of the 'internal rotational cooling' and 'internal rotational heating' rates for the OH^- as the collision energies are increased up to about 3000 cm^{-1} and therefore the corresponding rates could be evaluated up to the temperatures reached by the earlier experimental findings in the literature. Our present *ab initio* calculations found the state-changing rates to exhibit a rather slow dependence on the temperatures and that they invariably remain smaller than the usual estimates from the Langevin models. The latter model simply treats the overall reactivity as being driven by the atomic polarisability and by the long-range charge-polarisation potential: our present analysis is obviously more sophisticated in selecting the interaction forces between partners and in treating the inelastic dynamics. As should be expected, [15], the Langevin rates constitute the upper limit to the more realistic calculations of the present study. Furthermore, we found that simple evaluations of global rotational de-excitation rates or of rotational excitation rates at temperatures up to 450 K indicate the efficiencies of the collisional state-changing processes to be fairly large and to be comparable in size with the loss rates found in the experiments [15]. This datum should suggest that the de-excitation processes could translationally 'heat' preferentially the lighter partner in the trap and thus also contribute to the observed trap losses of the molecular anion. In conclusion, the quantum calculations presented by this work have clearly shown that the efficiency of rotational state-changing processes for both OH^- and OD^- molecular anions in collision with cold Rb atoms under the kinematic conditions of an ion trap can be very large and therefore likely to allow, at the lowest temperatures expected in the trap (<40 K) by current experiments, that both molecular isotopic variants to be de-excited to their lowest rotational levels on a time scale possibly shorter than the rates for actual molecular losses occurring in the trap.

Acknowledgments

We are grateful to the Computing Center of the University of Innsbruck for the availability of computational time in order to carry out the present work. The scientific project that includes the present investigation has been supported by the Austrian Science Fund (FWF), project P27047-N20. LGS also thanks the Spanish Ministry of Science and Innovation under grant CTQ2012-37404-C02–02.

References

[1] Carr L, Mille D D, Krems R and Ye J 2009 *New J. Phys.* **11** 055049
[2] Krems R 2008 *Phys. Chem. Chem. Phys.* **10** 4079
[3] Bodo E and Gianturco F 2006 *Rev. Phys. Chem.* **25** 313
[4] Loh H, Cossell K, Gran M, Ni K K, Meger E, Ye J B J and Cornell E 2013 *Science* **342** 1220
[5] Andre A, Mille D D, Doyle J, Lukin M, Maxwell S, Rabl P, Schoelkopf R and Zoller P 2006 *Nat. Phys.* **2** 636
[6] Ratschbache L, Zipkes C, Sias C and Köhl M 2012 *Nat. Phys.* **8** 649
[7] Gerlich D, Jusko P, Roucha S, Plasil I Z R and Glosik J 2012 *Astrophys. J.* **749** 22
[8] Hansen A K, Versolato O O, Kłosowski L, Kristensen S B, Gingell A, Schwarz M, Windberger A, Ulrich J, López-Urrutia J C and Drewsen M 2014 *Nature* **508** 76
[9] Staanum P, Højbjerre K, Skyt P, Hansen A and Drewsen M 2010 *Nat. Phys.* **6** 271
[10] Schneider T, Roth B, Duncker H, Ernsting I and Schiller S 2010 *Nat. Phys.* **6** 275
[11] Gerlich D, Plašil R, Zymak I, Hejduk M, Jusko P, Mulin D and Glosik J 2013 *J. Phys. Chem.* A **117** 10068
[12] Pearson J C, Oesterling L C, Herbst E and Lucia F C D 1995 *Phys. Rev. Lett.* **75** 2940
[13] Hudson E R 2009 *Phys. Rev.* A **79** 032716
[14] Rellergert W G, Sullivan S T, Schowalter S J, Kotochigova S, Chen K and Hudson E R 2013 *Nature* **495** 490
[15] Deiglmayr J, Göritz A, Best T, Weidemüller M and Wester R 2012 *Phys. Rev.* A **86** 043438
[16] Hauser D, Lee S, Carelli F, Spieler S, Lakhmanskaya O, Enders E, Kumar S, Gianturco F and Wester R 2015 *Nat. Phys.* **11** 467
[17] Wester R and Weidemueller M 2015 private communication
[18] González-Sánchez L, Carelli F, Gianturco F and Wester R 2015 *Chem. Phys.* **462** 111
[19] Gonzalez-Sanchez L, Tacconi M, Bodo E and Gianturco F 2008 *Eur. Phys. J.* D **49** 85–92
[20] Lim I, Schwerdtfeger P, Metz B and Stoll H 2005 *J. Chem. Phys.* **122** 104103

[21] Boys S F and Bernardi F 1970 *Mol. Phys.* **19** 553
[22] Molof R, Schwartz H, Miller T and Bederson B 1974 *Phys. Rev.* A **10** 1131
[23] Lopez-Duran D, Bodo E and Gianturco F 2008 *Comput. Phys. Commun.* **179** 821
[24] Martinazzo R, Bodo E and Gianturco F 2003 *Comput. Phys. Commun.* **151** 187
[25] Smith J, Kim J and Lineberger W 1997 *Phys. Rev.* A **55** 2036
[26] Lara M, Bohn J, Potter D, Sold a`n P and Hutson J 2006 *Phys. Rev. Lett.* **97** 183201
[27] Byrd J, Michels H Jr and Coté R J M 2013 *Phys. Rev.* A **88** 032710
[28] Caruso D, Tacconi M, Gianturco F and Yurtsever E 2012 *J. Chem. Sci.* **124** 93